Available online at www.sciencedirect.com
ScienceDirect
Journal of Magnetic Resonance 191 (2008) 304–314
JMR Journal of Magnetic Resonance
www.elsevier.com/locate/jmr

NMR study and quantum mechanical calculations on the 2-[(2-aminoethyl)amino]-ethanol–H_2O–CO_2 system

Jana P. Jakobsen, Eirik F. da Silva *, Jostein Krane, Hallvard F. Svendsen

Department of Chemical Engineering, Norwegian University of Science and Technology, 7491 Trondheim, Norway

Received 22 June 2007; revised 14 December 2007
Available online 9 January 2008

Abstract

^{13}C and ^{1}H NMR spectra were obtained for AEEA (2-[(2-aminoethyl)amino]-ethanol)–H_2O–CO_2 systems and quantum mechanical calculations were carried out for the different AEEA species. The results suggest that the main AEEA species under the conditions studied are free amine, primary carbamate, and secondary carbamate. There is also some indication that a dicarbamate species is formed, this species does however only appear to be formed in small amounts. Comparison between experimental data and quantum mechanical calculations suggest that most AEEA species take on conforms with some degree of intramolecular hydrogen bonding.

Keywords: CO_2 absorbent; NMR; Quantum mechanical calculations; Protonation shifts; Speciation

1. Introduction

Absorption is the most common industrial CO_2 capture technology today and recent studies suggest that the process will remain competitive also in the future [1]. However, there are still problems related to absorption technology such as the high financial cost, high energy requirements, and production of waste. Beside process design modifications and improvements, focus is turned towards the search for new solvents. A number of solvents have been studied in recent years by different research groups [2–6]. Reducing the overall energy consumption of the process, improving the kinetics and minimizing the waste production are key considerations in developing new solvent systems. A chemical to be used as a commercial absorbent must have high net cyclic capacity, high reaction rate for CO_2, and good chemical stability.

Recently, the diamine 2-[(2-aminoethyl)amino]-ethanol (AEEA) has been identified by Mamun et al. [7] as a new promising absorbent by a set of screening tests focusing on the absorption rate and capacity of the amines. It was shown that AEEA offers high absorption rate combined with high net cyclic capacity. The net cyclic capacity of AEEA is somewhat higher than that of MEA (the commonly used alkanolamine) and it maintains its absorption power at higher CO_2 concentrations. A reliable design of the process with the new solvent requires information on the solubility of CO_2 in the solvent and on the chemical equilibrium constants. Experimental determination and modeling of the solubility of CO_2 in 30% mass AEEA is the subject of a paper by Mamun et al. [8].

The objective of this work is the characterization of the chemical system AEEA–H_2O–CO_2 by use of experimental NMR spectroscopy and quantum mechanical calculations. The NMR spectra provide information on the hydrogen–carbon framework and allow us to identify the species present in the system. Determining the system speciation is very important for the establishment of reaction mechanisms and also for the thermodynamic modeling of the system that is necessary for simulation of the absorption process. The NMR spectra together with the quantum mechanical calculations may also provide insight into the molecular structure and stable conformer forms.

The research on CO_2 absorption technology has mainly been carried out in chemical engineering communities and

* Corresponding author. Fax: +47 352 392 8722.
E-mail address: Eirik.Silva@sintef.no (E.F. da Silva).

1090-7807/$ - see front matter © 2008 Elsevier Inc. All rights reserved.
doi:10.1016/j.jmr.2007.12.022

the focus has been on measuring equilibria, kinetics, and physical properties on solvent systems. Less work has been done on understanding the process at molecular level and only a few papers report NMR work on CO_2 absorption [9–16]. Several of these papers deal with solvents that have multiple amine functionalities.

2. Experimental method

^1H and ^{13}C spectroscopy was applied to investigate qualitatively the solutions of 5 wt% AEEA titrated with HCl or loaded with CO_2 at 20 °C. The XWINNMR software developed by BRUKER was used for data acquisition and processing. Spectra were acquired on 400 and 600 MHz BRUKER spectroscopes. The chemicals used were: AEEA of purity >97 mass% from Acros Organics and CO_2 gas of purity >99.99 mol% obtained from AGA Gas GmbH. Tetramethylsilane (TMS) was used as internal reference.

3. Computational details

Initial gas phase conformer searches for the various AEEA species were carried out at a molecular mechanics level (MMFF94 [17]). These calculations were performed with PC Spartan Pro version 1.0.7 [18]. From this initial conformer search the most stable conformers and conformers displaying different forms of hydrogen bonding were selected for NMR calculations.

The selected conformers were then optimized at B3LYP/6-311++G(d,p) level [19]. The NMR nuclear shieldings were computed by using gauge-invariant atomic orbitals (GIAO) at this level of theory. These calculations were performed with Gaussian 98 [20]. The chemical shifts were calculated with TMS as reference. The chemical shift of one AEEA conformer relative to TMS was calculated at MPW1PW91 level of theory with incorporation of solvent effects (details given in Supporting information); all other chemical shifts were calculated relative to this conformer (B3LYP level calculations used to determine relative shifts between AEEA conformers and species). The MPW1PW91 level has been reported to perform well in ^{13}C NMR calculations [21].

Free energies of solution of the various conformers have also been calculated. The solvation energy was calculated with single point IEFPCM [22] continuum model calculations on the B3LYP/6-311++G(d,p) geometries (IEFPCM/B3LYP/6-311++G(d,p)//B3LYP/6-311++G(d,p)). The IEFPCM calculations were carried out with their default settings in Gaussian 98. Such model solvation energies do have a certain uncertainty, for ions the error bars can be as high as ±3 kcal/mol. Such a model can however offer guidance on what conformers are likely to be stable in solution.

To assess the sensitivity of the results to the theoretical method applied some NMR calculations have also been carried out at the MPW1PW91/6-311+G(2d,p)-IEFPCM level (geometry optimized in solution).

The conformers will be indicated as WXYZ*abc*(*ij*). W, X, Y, and Z refer to the N_p-C_4-C_3-N_s dihedral, C_4-C_3-N_s-C_2, C_3-N_s-C_2-C_1, and Ns-C2-C1-O dihedrals, respectively, (the numbering of carbons is given in Fig. 1). *a* in the conformer notation refers to the *lp*N-N_p-C_4-C_3 dihedral and *b* to the *lp*N-N_p-C_2-C_1 dihedral, where *lp*N is the lone pair of electrons on the nitrogen atoms. *c* in the conformer notation is the C_3-C_4-O-H(O) dihedral angle. *i* and *j* indicate conformers of carbamate species: *i* being the C(CO_2)-N_p-C_4-C_3 dihedral and *j* is the C(CO_2)-N_s-C_2-C_1 dihedral. G or g will indicate a gauche(+) conformer, G′ or g′ will indicate a gauche(−) conformer, finally a T or t will indicate a trans conformer. For species with no *lp*N at a given site this will be indicated with a "−".

4. Chemical system

AEEA is a diamine and while the nature of reactions is likely to be the same as for molecules with single amine functionality there is a greater number of species that can be formed (Versteeg et al. [23] have reviewed the chemical reactions of CO_2 absorption). The species formed by AEEA are likely to be the same as formed by other diamine molecules such as piperazine. The two amine sites are however nonequivalent in AEEA, adding to the number of nonequivalent species formed. The following 14 species are expected to exist in the liquid phase: AEEA, $AEEAH^+$, $AEEAH_2^{+2}$, $AEEACOO_p^-$, $AEEACOO_s^-$, $AEEACO_{2p}H$, $AEEACO_{2s}H$, $AEEA(CO_2)^{-2}$, CO_2, HCO_3^-, CO_3^{-2},

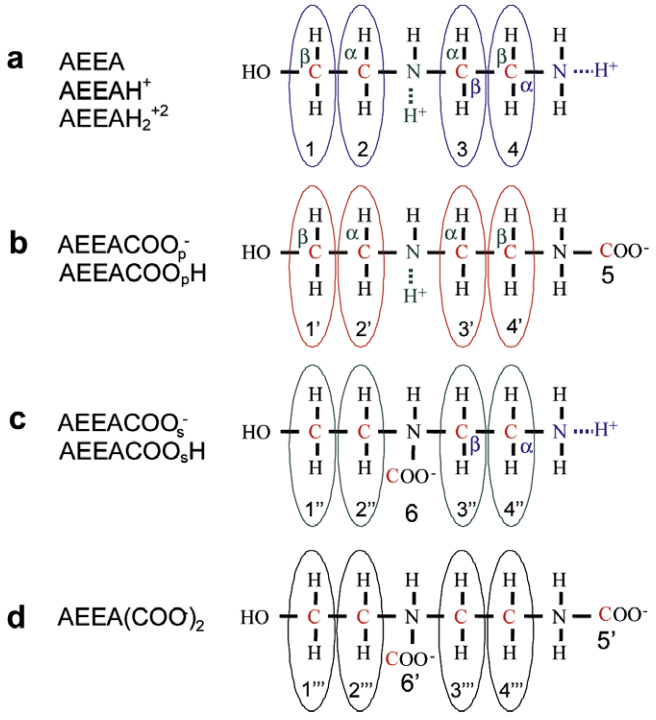

Fig. 1. Molecular structures and type of nuclei in AEEA species.

H_2O, H_3O^+, and OH^-. Subscript p is used to indicate CO_2 group bonding to the primary amine group, while subscript s indicates bonding to the secondary amine group.

The expected chemical equilibrium reactions are as follows:

Protonation of AEEA:

$$AEEA + H_3O^+ \Longleftrightarrow AEEAH^+ + H_2O \quad (1)$$

Diprotonation of AEEA:

$$AEEAH^+ + H_3O^+ \Longleftrightarrow AEEAH_2^{+2} + H_2O \quad (2)$$

Formation of carbamate on primary and secondary amine functionality:

$$AEEA + CO_2 + H_2O \Longleftrightarrow AEEACOO_p^- + H_3O^+ \quad (3)$$

$$AEEA + CO_2 + H_2O \Longleftrightarrow AEEACOO_s^- + H_3O^+ \quad (4)$$

Carbamate protonation:

$$AEEACOO_p^- + H_3O^+ \Longleftrightarrow AEEACOO_pH + H_2O \quad (5)$$

$$AEEACOO_s^- + H_3O^+ \Longleftrightarrow AEEACOO_sH + H_2O \quad (6)$$

Formation of dicarbamate:

$$AEEACOO_p^- + CO_2 + H_2O \Longleftrightarrow AEEA(COO)_2^{-2} + H_3O^+ \quad (7)$$

$$AEEACOO_s^- + CO_2 + H_2O \Longleftrightarrow AEEA(COO)_2^{-2} + H_3O^+ \quad (8)$$

The molecular structure and assignment of proton/carbon type of nuclei in the expected amine species are shown in Fig. 1.

5. Results and discussion

5.1. Titration experiments—protonation shifts

Five wt% AEEA solution was titrated with HCl. ^1H and ^{13}C spectra were acquired for the samples at various pH. The ^{13}C and ^1H spectra obtained for pure AEEA (without any HCl) are shown in Figs. 2 and 3, respectively.

It is not possible to distinguish between the two species AEEA and $AEEAH^+$ due to the fast proton exchange with water. The peaks in the spectra represent both the AEEA and $AEEAH^+$ and the chemical shift of the peaks represents the average of the chemical shifts of AEEA and $AEEAH^+$. The actual chemical shift corresponds to the relative ratio of these species in solution and therefore changes according to the pH. In the acid free solution, mainly the free amine is assumed to be present so the chemical shifts in the spectra in Figs. 2 and 3 correspond to the free amine shifts. Upon addition of HCl (decreasing pH) the fraction of protonated amine increases and the peaks drift towards the chemical shifts of the protonated amine. The peaks H2 and H3 exchanged positions in the spectra as the titration proceeded. The particular chemical shifts as function of pH are given in the Supporting information. The relative change in the chemical shifts with respect to the shifts in pure AEEA as function of pH is shown for the carbon and proton peaks in Figs. 4 and 5, respectively.

The curves in Figs. 4 and 5 represent titration curves for the four types of carbon/proton types. AEEA is a diamine with one primary and one secondary amine group and has therefore two equilibrium points (EPs) corresponding to the formation of protonated and diprotonated AEEA. These two equivalence points are clearly visible on the titration curves. The absolute difference in the chemical shifts defined as $(\delta_{\text{protonated amine}} - \delta_{\text{free amine}})$ is called protonation shift. For AEEA we can distinguish two protonation shifts, the first protonation shift is defined as $(\delta_{\text{single protonated amine}} - \delta_{\text{free amine}})$ and the second protonation shift as $(\delta_{\text{double protonated amine}} - \delta_{\text{single protonated amine}})$. The two protonation shifts together with the overall protonation shift $(\delta_{\text{double protonated amine}} - \delta_{\text{free amine}})$ are listed for carbon and proton in Tables 1 and 2, respectively.

5.2. Experiments with loaded samples

Experiments with CO_2 loaded AEEA solutions were performed with loadings of 0.2, 0.5, and 0.8. ^1H and ^{13}C

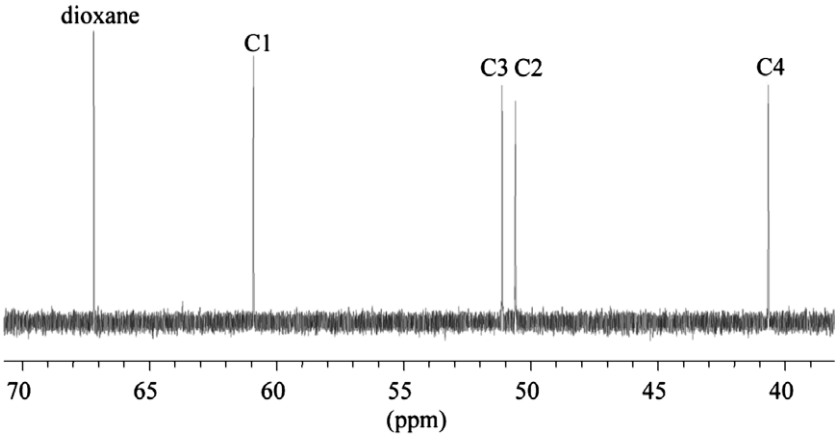

Fig. 2. ^{13}C spectrum of 5 wt% AEEA solution.

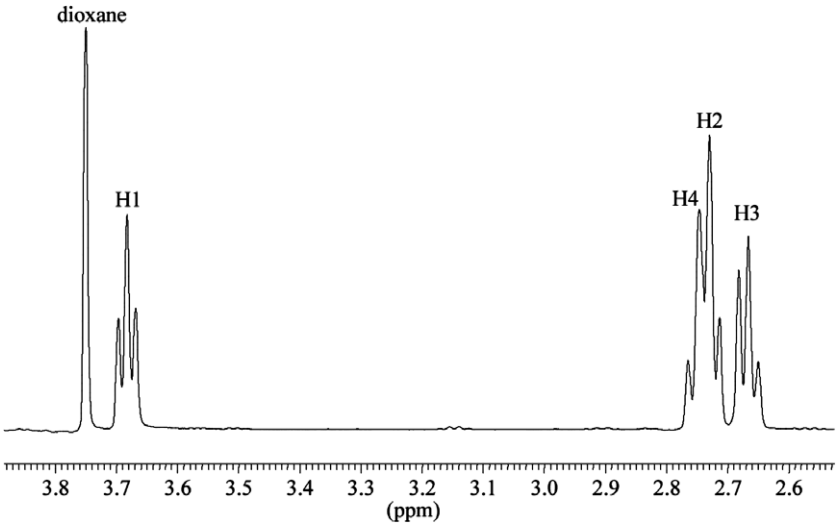

Fig. 3. ^{1}H spectrum of 5 wt% AEEA solution.

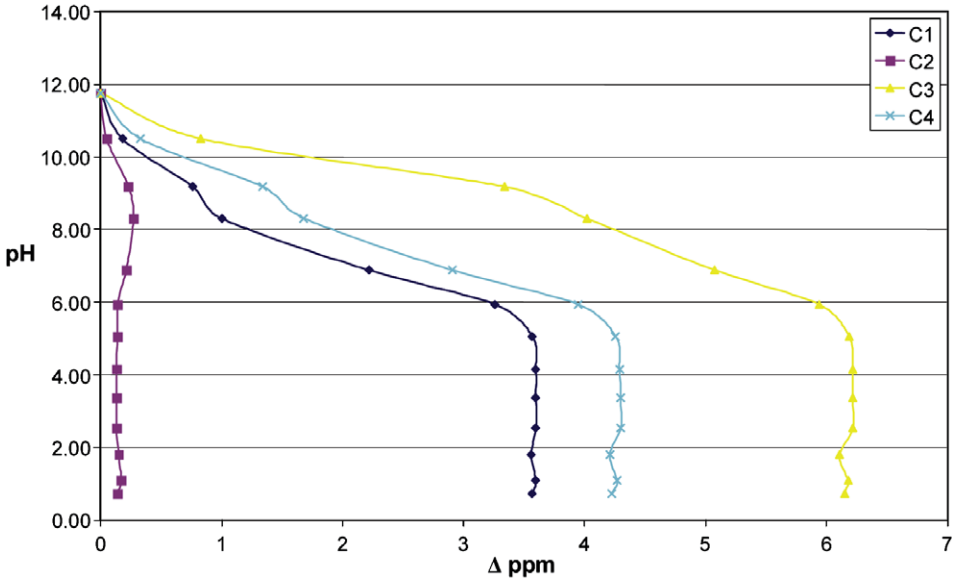

Fig. 4. Titration curves of AEEA; the chemical shifts of ^{13}C peaks as function of pH.

spectra were acquired. The loading is the molar ratio of absorbed CO_2 to amine concentration. In addition, 2D spectra ($^{1}H/^{13}C$ and $^{1}H/^{1}H$) were acquired in order to assign the peaks properly to the particular nuclei. Because of the fast exchange of protons, carbamate species cannot be distinguished from the protonated forms of carbamate in the NMR spectra.

Three main components were identified in the loaded solutions. We believe these to be amine, primary carbamate, and secondary carbamate. Additional peaks were also registered (only in ^{13}C) that are attributed to dicarbamate. The molecular formulae of these species and the nuclei assignment are illustrated in Fig. 1. 3×4 peaks were found in the high field region for the four proton/carbon types in the three species and their protonated forms, see Figs. 6 and 8. In the low field region of the ^{13}C spectra (Fig. 7) the peaks for the primary and secondary carbamate (CO_2^-) groups were found and the common peak for carbonate/bicarbonate. The peaks were assigned to the particular carbon/proton groups with help of the 2D spectra, see Fig. 9. The registered chemical shifts in ppm are summarized in Tables 3 and 4.

5.3. Species distribution

The relative integral areas of the peaks correspond to relative species concentrations. The spectra of loaded samples were fitted in IGORPro and the peak areas were integrated for the three main components. The distribution between the three amine species was expressed as fractions of the total amine concentration. The relative AEEA

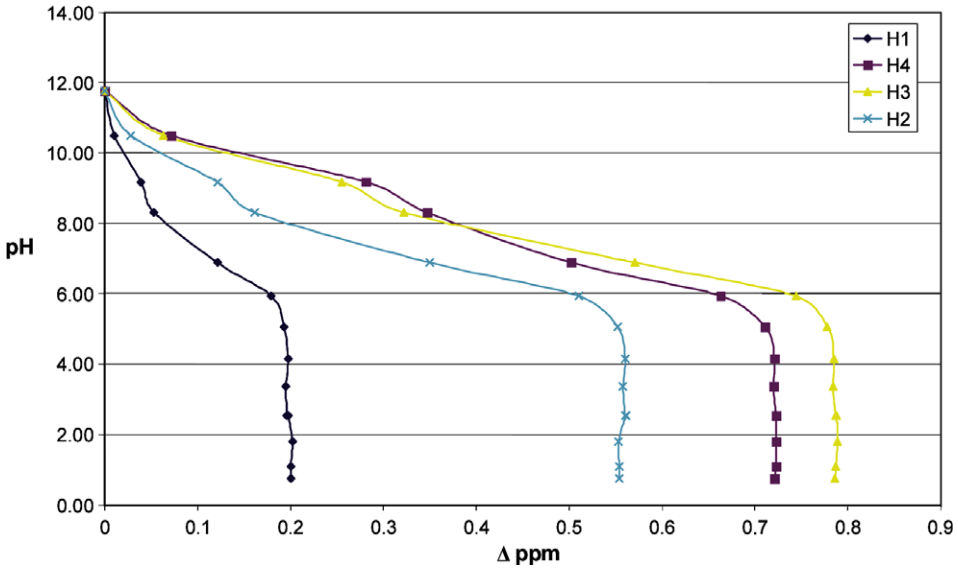

Fig. 5. Titration curves of AEEA; the chemical shifts of ^{1}H peaks as function of pH.

Table 1
^{13}C protonation shifts

	C1	C2	C3	C4
First protonation	−1	−0.27	−4.02	−1.68
Second protonation	−2.57	+0.13	−2.13	−2.55
Overall shift	−3.57	−0.14	−6.15	−4.23

Table 2
^{1}H protonation shifts

	H1	H2	H3	H4
First protonation	−0.053	−0.161	−0.322	−0.347
Second protonation	−0.147	−0.393	−0.464	−0.374
Overall shift	−0.2	−0.554	−0.786	−0.721

species concentrations are plotted against "experimental" CO_2 loading (based on the NMR results) in Fig. 10.

5.4. Computational results

For each chemical species the conformer populations were estimated. The populations were optimized to give the best agreement with experimental chemical shifts. The different AEEA species have a high number of conformers and calculations have been carried out for only some of these. The most stable conformers identified for each species are shown in Fig. 11. In addition to the conformers identified as the most stable ones, conformers with different forms of hydrogen bonding have been studied.

In Fig. 12 is shown $^{1}H/^{13}C$ spectra based on the B3LYP/6-311++G(d,p) chemical shifts and the estimated conformer populations. The full set of data is given in the Supporting information. In creating this figure it was assumed that no protonated carbamate was formed. We currently believe carbamate molecules to be weak bases, but further studies will be required to ascertain this.

Comparing Fig. 12 with Fig. 9 we can see that the calculated spectra captures most of the features in the experimental spectra. Most of the chemical shifts are also in reasonably good agreement. The present calculations do have a number of limitations; B3LYP level chemical shifts are not entirely accurate, solvation effects are not accounted for and a limited number of conformers have been studied. Given these limitations, full quantitative agreement between experiment and calculations cannot be expected. Comparison between B3LYP and MPW1PW91 results (shown in Supporting information) suggest that changing the level of theory can change chemical shifts by several ppm, results at the different levels of theory are however similar.

From the fitting of conformer populations we can draw some tentative conclusions on the conformers formed and the nature of hydrogen bonding. For AEEA itself the spectra can be accounted for by a G′TTG′*ggg* conformer having two intramolecular hydrogen bonds. The difference in spectra between different conformers is however too small to draw confident conclusions.

A main feature of the protonated AEEA signals is the large relative shift between the C2 and C3 ^{13}C signals. Only a few conformers display such a large relative difference in these signals. The results are consistent with G′G′TG-*gt* being one of the dominant conformer of protonated AEEA. This would suggest that protonation on the primary amine site is dominating. The same conformer also gives reasonable agreement with the proton spectra.

For the primary carbamate species best agreement was obtained with a TG′TGtg′g′(g) conformer having no intramolecular bonding at the carbamate functionality.

For secondary carbamate form the agreement between experimental and calculated spectra is relatively poor, no conformer spectra being very close to the experimental one. This discrepancy may perhaps be the result of failure

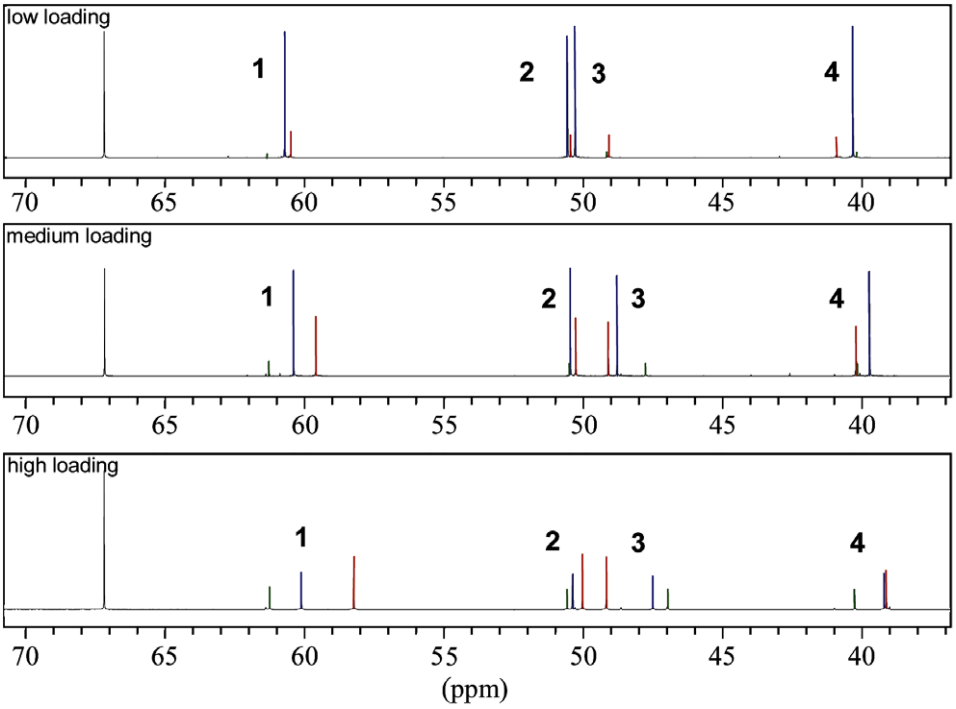

Fig. 6. The 1D carbon spectra of loaded samples (blue: AEEA/AEEAH$^+$, red: AEEA-COO$_p^-$/H$^+$, green: AEEA-COO$_s^-$/H$^+$). (For interpretation of the references to colour in this figure legend, the reader is referred to the web version of this article.)

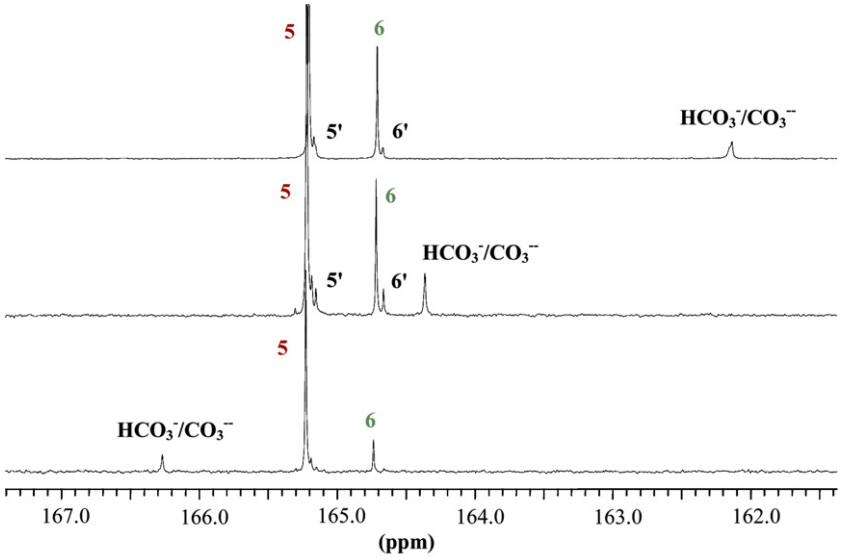

Fig. 7. The low field part of the ^{13}C spectra.

to include solvation effects in the calculations or failure to identify the most stable conformers. It may also be that there is a significant component of protonated carbamate. Given this level of uncertainty it is hard to draw conclusions on the conformer form of secondary carbamate species.

The ^{13}C spectra for dicarbamate species have two separate but close peaks for the CO_2 groups (Supporting information). The data also indicate that these dicarbamate peaks may well overlap with the peaks of CO_2 groups of primary or secondary dicarbamate. This suggests that the small peaks observed in Figs. 6 and 7 may well be a dicarbamate species.

The conformer populations suggested by comparison between experimental chemical shifts and chemical shifts determined from quantum mechanical calculations are in reasonable overall agreement with the relative free energies in solution that have been calculated. Most of the conformers that we suggest to be populated are among the more stable in terms of free energy in solution. Over-

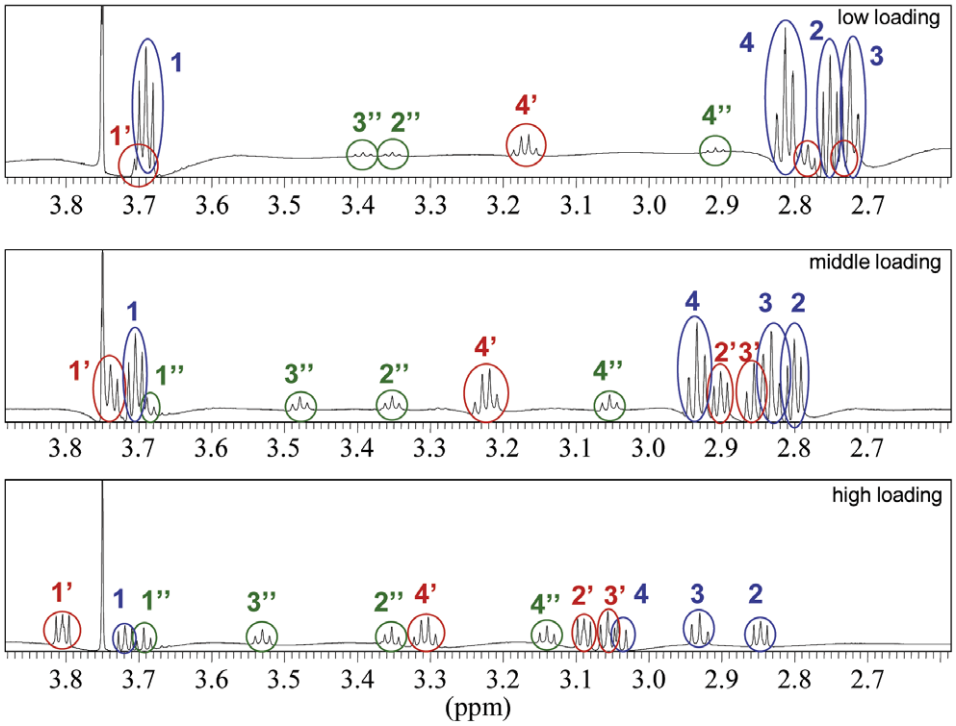

Fig. 8. The 1D proton spectra of loaded samples (blue: AEEA/AEEAH$^+$, red: AEEA-COO$_p^-$/H$^+$, green: AEEA-COO$_s^-$/H$^+$). (For interpretation of the references to colour in this figure legend, the reader is referred to the web version of this article.)

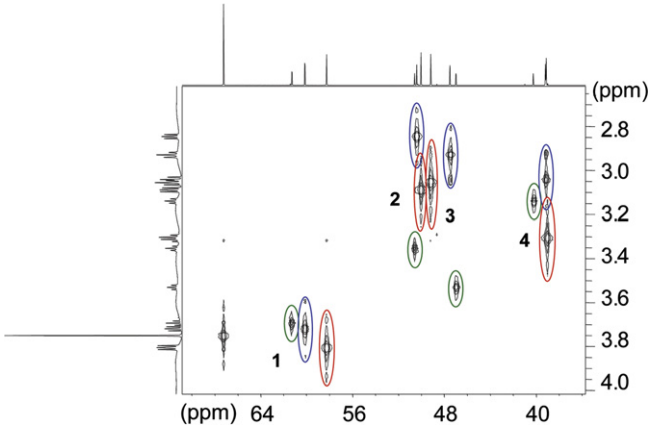

Fig. 9. ^{1}H/^{13}C spectra at the highest loading (blue → AEEA/AEEAH$^+$, red → AEEA-COO$_p^-$/H$^+$, green → AEEA-COO$_s^-$/H$^+$). (For interpretation of the references to colour in this figure legend, the reader is referred to the web version of this article.)

Table 3
^{13}C shift in ppm

	α_{CO_2}	C1	C2	C3	C4	CO_2^-
AEEA	0.2	60.22	49.74	50.01	39.70	—
	0.5	59.89	49.89	48.21	39.08	—
	0.8	59.76	49.98	47.06	38.71	—
AEEACO$_{2p}^-$	0.2	60.01	49.89	48.51	40.29	165.38
	0.5	59.09	49.70	48.52	39.56	165.35
	0.8	57.87	49.61	48.75	38.64	165.50
AEEACO$_{2s}^-$	0.2	60.87	50.01	48.58	39.58	164.88
	0.5	59.87	49.89	47.18	39.59	164.84
	0.8	60.91	50.16	46.54	39.77	165.0

Table 4
^{1}H shift in ppm

	α_{CO_2}	H1	H2	H3	H4
AEEA	0.2	3.69	2.72	2.75	2.81
	0.5	3.71	2.80	2.83	2.94
	0.8	3.72	2.85	2.93	3.04
AEEACO$_{2p}^-$	0.2	3.70	2.78	2.73	3.17
	0.5	3.74	2.90	2.86	3.22
	0.8	3.81	3.09	3.06	3.31
AEEACO$_{2s}^-$	0.2	3.68	3.35	3.39	2.91
	0.5	3.69	3.35	3.48	3.06
	0.8	3.69	3.35	3.53	3.14

all this would suggest that our conformer assignment is plausible, but uncertain. More confident assignment can perhaps be achieved by high level chemical shift calculations that take into account solvation effects and further work on determining the solvation energy of different conformers.

5.5. Protonation shifts

From Figs. 4 and 5, it can be seen that the change in ^{13}C and ^{1}H chemical shifts due to the protonation on nitrogen is different for the various carbon/proton types in the AEEA molecule. According to our experimental experience, the protonation on the nitrogen atom has a major effect on the carbon in β-position and the proton in α posi-

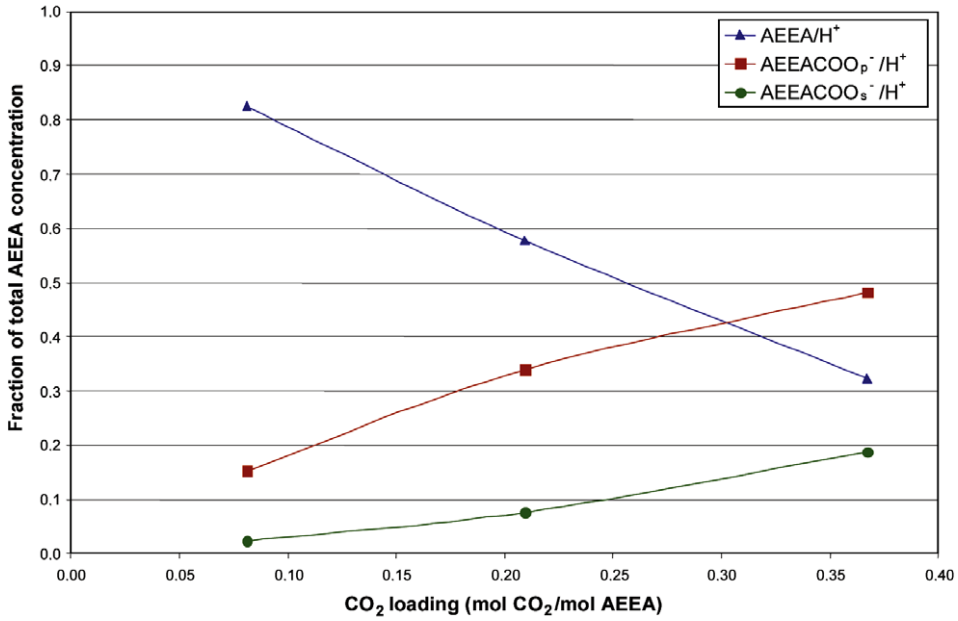

Fig. 10. The relative AEEA species distribution.

tion to that nitrogen. In the first protonation stage, the protons will associate with both the primary and secondary amine group in a certain ratio which cannot be determined from the experiments, but is assumed to be 80–90% with the primary group. This assumption, that the first protonation involves mainly the primary nitrogen group, is supported by the fact that the first protonation shift is largest for C3 and H4, i.e., the β-carbon and α-proton related to the primary nitrogen, respectively. Similarly, in the second protonation stage the protons may associate with both the primary or secondary group depending on where the first protonation took place. Since the majority of AEEA molecules are assumed to be protonated on primary nitrogen group in the first stage, the second protonation can be associated with protonation on the secondary nitrogen group. A second inversion point corresponding to the second protonation occurs at lower pH values. There the shift is largest for the β-carbons C1 and C4 and the α-proton H3 related to the secondary nitrogen group.

As seen in Table 1, the overall pH shift was largest for carbon C3, which is in β-position with respect to the primary nitrogen group and in α-position with respect to the secondary nitrogen group. The second largest pH shift was the pH shift of carbon C4, which is in α-position with respect to the primary nitrogen group and in β-position with respect to the secondary nitrogen group. The shift of carbon C1, which is in β-position with respect to the secondary nitrogen group was a bit smaller than for carbon C4 and the smallest pH shift was identified for carbon C2, which is in α-position with respect to the secondary nitrogen group.

The chemical shift is reflecting the chemical/electronic environment, i.e., the shielding of a given carbon nuclei. Many different factors like: hybridization, inductive effects of substituents, steric effects, and electric field effects all combine in a nontrivial way to the shielding of a ^{13}C nucleus. These effects often compete and it is very difficult to separate their individual contributions from each other. For open-chain molecules, the interpretation of ^{13}C shifts is also complicated by the conformational mobility since the chemical shift is often an average of differently populated conformers.

5.6. Comparison with N-propyl-1,2-ethanediamine

An experimental study on ^{13}C NMR protonation shifts of aqueous amines was performed by Sarneski et al. [24] A correlation was constructed to calculate the protonation shifts based on parameters that were obtained by regression analysis of the experimental protonation data. For diamine molecules the protonation was calculated as a linear sum of contributions from protonation of each amino group. The correlation proposed by Sarneski et al. was applied to estimate the protonation shifts of $CH_3CH_2CH_2NHCH_2CH_2NH_2$, a diamine similar to AEEA, but with the OH group exchanged by CH_3. The effect of OH on the protonation shifts is in this case not accounted for. Protonation shifts for $CH_3CH_2CH_2NHCH_2CH_2NH_2$ estimated by the correlation of Sarneski et al., the experimental values for the diamine $CH_2CH_2NHCH_2CH_2NH_2$ and the experimental values obtained in this work for AEEA are summarized in Table 5.

The results show significant similarity in the protonation shift between the two molecules, most of the shifts having the same sign and roughly the same magnitude.

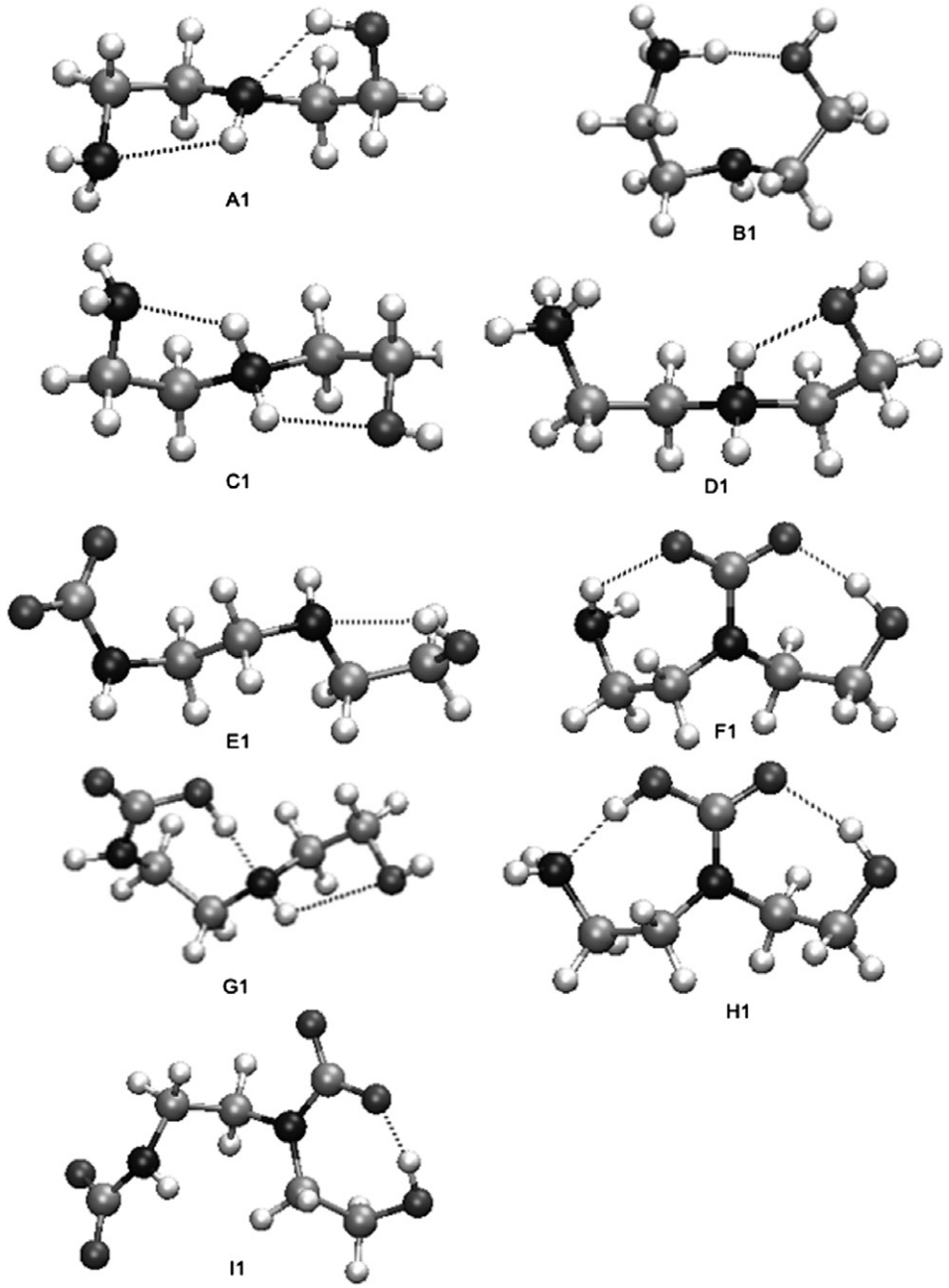

Fig. 11. B3LYP/6-311++G(d,p) geometries of different AEEA species. A1: AEEA. B1: $AEEAH^{+}$ (primary protonation). C1: $AEEAH^{+}$ (secondary protonation). D1: $AEEAH_2^{+2}$. E1: $AEEACOO_p^{-}$. F1: $AEEACOO_s^{-}$. G1: $AEEACOO_pH$. H1: $AEEACOO_sH$. 11: $AEEA(COO^{-})_2$.

5.7. Effect of CO_2 loading

The effect of loading on the ^{13}C and ^{1}H spectra can be seen in Figs. 6 and 8. The figures show the ^{1}H spectra and the high field part of the ^{13}C spectra (peaks representing the amine carbons) for 5 wt% AEEA solution with different CO_2 loadings. At the lowest loading the concentration of amine is highest but there are also peaks for primary carbamate and very small peaks for secondary carbamate. The amine gets depleted by the reaction with CO_2 while the concentrations of primary and secondary carbamate increase with increasing loading. At the highest loading the concentration of primary carbamate is highest and there are also detected peaks that can be assigned to dicarbamate.

As in the case of AEEA, the nitrogen groups in the AEEA-carbamates are protonated and we cannot distinguish in the NMR spectra between the species and their protonated form because the proton exchange is fast with respect to the NMR time scale. Therefore, the integrated peak areas represent the concentration of both forms. The peak position is an average and change with pH according to the relative ratio of the two forms. In AEEA both N-groups can be protonated, whereas in primary $AEEACOO^{-}$ it is the secondary N-group and in secondary $AEEACOO^{-}$ it is the primary group that becomes

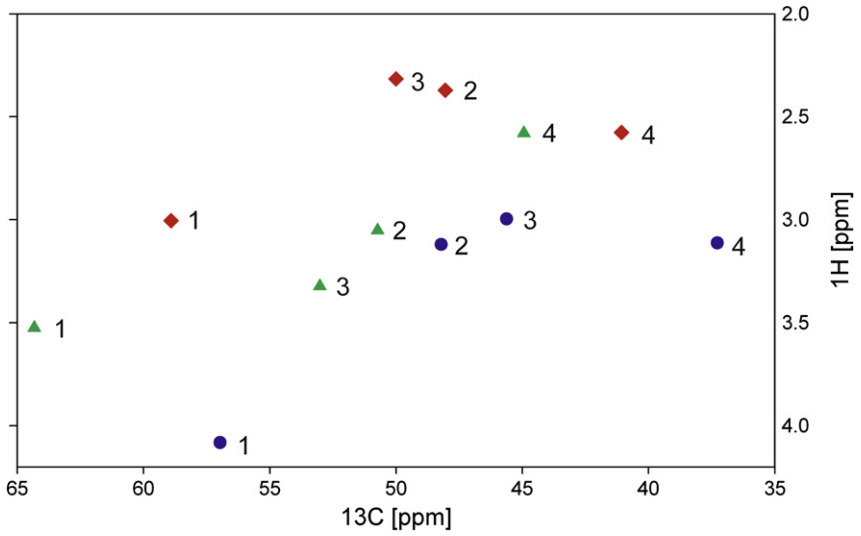

Fig. 12. $^{1}H/^{13}C$ spectra based on calculated chemical shifts at B3LYP/6-311++G(d,p) level with averaging over conformers. Blue → AEEA/AEEAH^{+}, red → AEEA-COO$_p^{-}$/H^{+}, green → AEEA-COO$_s^{-}$/H^{+}. (For interpretation of the references to colour in this figure legend, the reader is referred to the web version of this article.)

Table 5
Protonation shifts obtained experimentally, estimated by an empirical formula

δ protonation [ppm]	C1	C2	C3	C4
Exp. this work $HOCH_2CH_2NHCH_2CH_2NH_2$				
1equi	−1	−0.27	−4.02	−1.68
2equi	−2.57	+0.13	−2.13	−2.55
Overall	−3.57	−0.14	−6.15	−4.23
Exp. Sarneski et al. [24] $CH_3CH_2NHCH_2CH_2NH_2$				
1equi	−2.53	−0.37	−2.65	−2.78
2equi	−0.83	+0.65	−4.55	−1.88
Overall	−3.36	+0.28	−7.2	−4.66
Estimated by Sarneski et al. [24] $CH_3CH_2CH_2NHCH_2CH_2NH_2$				
1equi	−2.01	−2.44	−4.59	−2.01
2equi	−3.26	−1.54	−1.54	−3.26
Overall	−5.27	−3.98	−6.13	−5.27

protonated. Therefore, different carbons are affected in the three species. The overall (from low to high loading) pH shifts are summarized for ^{13}C in Table 6 and for ^{1}H in Table 7. The effect of pH on the protonation of the amine groups in AEEA was already discussed for the titration spectra. In the case of primary carbamate where the secondary amine-group is protonated the shift was largest on the carbons C1 and C4 (α-position) and protons H2 and H3 (β-position). In the secondary carbamate the protonated group is the primary amine-group and the most affected carbon was therefore carbon C3 (β-position) and the most affected proton was H4 (α-position).

Table 6
Overall Δ shift of peaks in ^{13}C spectra

$\Delta\delta$ [ppm]	C1	C2	C3	C4
AEEA	−0.46	−0.03	−2.67	−0.99
AEEAprimCOO^{-}	−2.15	−0.28	+0.23	−1.65
AEEAsecCOO^{-}	+0.03	+0.13	−2.04	+0.19

Table 7
Overall Δ shift of peaks in ^{1}H spectra

$\Delta\delta$ [ppm]	H1	H2	H3	H4
AEEA	−0.03	−0.10	−0.21	−0.23
AEEAprimCOO^{-}	−0.11	−0.31	−0.33	−0.14
AEEAsecCOO^{-}	−0.02	0	−0.14	−0.23

6. Conclusion

NMR spectra were acquired and quantum mechanical chemical shifts for the AEEA–H_2O–CO_2 system were obtained. Three major species were identified in the system at conditions studied: AEEA, AEEACOO$_p^{-}$, and AEEACOO$_s^{-}$. It also seems probable, but less certain, that a dicarbamate species is present in the system. Comparison between experimental and quantum mechanical spectra suggest that most species are populated by conformers with some degree of intramolecular hydrogen bonding. The relative species distribution in the system was calculated based on the peak integral areas. The results obtained in this work represent additional information on the chemical system AEEA–H_2O–CO_2 and will be used to design the absorption process for CO_2 capture with the new solvent AEEA. The speciation data can be in particular important for modeling of chemical and phase equilibria of the AEEA–H_2O–CO_2 system, where the most important task will be determining the carbamate stability constants for this molecule.

Appendix A. Supplementary data

Supplementary data associated with this article can be found, in the online version, at doi:10.1016/j.jmr.2007.12.022.

References

[1] H.M. Kvamsdal, K. Jordal, O. Bolland, Energy 32 (2007) 10–24.
[2] T. Mimura, S. Satsumi, M. Iijima, S. Mitsuoka, Greenhouse Gas Control Technologies, Elsevier, 1999, pp. 71–76.
[3] A. Chakma, P. Tontiwachiwuthikul, Greenhouse Gas Control Technologies, Elsevier, 1999, pp. 35–42.
[4] D. Bonenfant, M. Mimeault, R. Hausler, Ind. Eng. Chem. Res. 42 (2003) 3179–3184.
[5] P. Singh, J.P.M. Niederer, G.F. Versteeg, in: Eighth International Conference on Greenhouse Gas Control Technologies, Trondheim, Norway, 2006.
[6] L. Hakka, M.A. Ouimet, Method for recovery of CO_2 from gas streams, US patent application 2004/0253159, 2004.
[7] S. Ma'mun, H.F. Svendsen, K.A. Hoff, O. Juliussen, in: Seventh International Conference on Greenhouse Gas Control Technologies, vol. I, 2005, pp. 45–53.
[8] S. Ma'mun, J.P. Jakobsen, O. Juliussen, H.F. Svendsen, Ind. Eng. Chem. Res. 45 (2006) 2505–2512.
[9] S. Bishnoi, G.A. Rochelle, Chem. Eng. Sci. 55 (2000) 5531–5543.
[10] S. Bishnoi, G.T. Rochellle, Ind. Eng. Chem. Res. 41 (2002) 604–612.
[11] J.T. Cullinane, G.T. Rochelle, Fluid Phase Equilib. 227 (2005) 197–213.
[12] A.K. Chakraborty, G. Astarita, K.B. Bischoff, Chem. Eng. Sci. 41 (1986) 997–1003.
[13] J.Y. Park, S.J. Yoon, H. Lee, Environ. Sci. Technol. 37 (2003) 1670–1675.
[14] T. Suda, T. Iwaki, T. Mimura, Chem. Lett. 9 (1996) 777–778.
[15] J.P. Jakobsen, J. Krane, H.F. Svendsen, Ind. Eng. Chem. Res. 44 (2005) 9894–9903.
[16] A. Hartono, E.F. da Silva, H. Grasdalen, H.F. Svendsen, Ind. Eng. Chem. Res. 46 (2007) 249–254.
[17] T.A.J. Halgren, Comp. Chem. 17 (1996) 490–519.
[18] PC SPARTAN Version 1.0.7, Wavefuncion, Inc., 18401 Von Karmen Ave. #370 Irvine, CA 92715, USA.
[19] A.D. Becke, J. Chem. Phys. 98 (1993) 5648–5652.
[20] M.J. Frisch, G.W. Trucks, H.B. Schlegel, G.E. Scuseria, M.A. Robb, J.R. Cheeseman, V.G. Zakrzewski, J.A. Montgomery, Jr., R.E. Stratmann, J.C. Burant, S. Dapprich, J.M. Millam, A.D. Daniels, K.N. Kudin, M.C. Strain, O. Farkas, J. Tomasi, V. Barone, M. Cossi, R. Cammi, B. Mennucci, C. Pomelli, C. Adamo, S. Clifford, J. Ochterski, G.A. Petersson, P.Y. Ayala, Q. Cui, K. Morokuma, D.K. Malick, A.D. Rabuck, K. Raghavachari, J.B. Foresman, J. Cioslowski, J.V. Ortiz, A.G. Baboul, B.B. Stefanov, G. Liu, A. Liashenko, P. Piskorz, I. Komaromi, R. Gomperts, R.L. Martin, D.J. Fox, T. Keith, M.A. Al-Laham, C.Y. Peng, A. Nanayakkara, M. Challacombe, P.M.W. Gill, B. Johnson, W. Chen, M.W. Wong, J.L. Andres, C. Gonzalez, M. Head-Gordon, E.S. Replogle, J.A. Pople, Gaussian 98, Revision A.9, Gaussian, Inc., Pittsburgh PA, 1998.
[21] K.B. Wiberg, J. Comp. Chem. 20 (1999) 1299–1333.
[22] M.T. Cances, V. Mennucci, J. Tomasi, Chem. Phys. 107 (1997) 3032–3041.
[23] G.F. Versteeg, L.A.J. van Dijck, W.P.M. van Swaaij, Chem. Eng. Commun. 144 (1996) 113–158.
[24] J.E. Sarneski, H.L. Surprenant, F.K. Molen, C.N. Reilley, Anal. Chem. 47 (13) (1975) 2116–2124.